Lauer, Kevin; Brokmann, Geert; Bähr, Mario; Ortlepp, Thomas

Determination of piezo-resistive coefficient π44 in p-type silicon by comparing simulation and measurement of pressure sensors

Original published in:	AIP Advances / American Institute of Physics. - New York, NY : American Inst. of Physics. - 11 (2021), 8, art. 085005, 6 pp.
Original published:	2021-08-03
ISSN:	2158-3226
DOI:	10.1063/5.0060034
[*Visited:*	2022-03-02]

Determination of piezo-resistive coefficient π_{44} in *p*-type silicon by comparing simulation and measurement of pressure sensors

Cite as: AIP Advances 11, 085005 (2021); doi: 10.1063/5.0060034
Submitted: 15 June 2021 • Accepted: 19 July 2021 •
Published Online: 3 August 2021

Kevin Lauer,[1,2,a] Geert Brokmann,[1] Mario Bähr,[1] and Thomas Ortlepp[1]

AFFILIATIONS

[1] CiS Forschungsinstitut für Mikrosensorik GmbH, Konrad-Zuse-Str. 14, 99099 Erfurt, Germany
[2] TU Ilmenau, Institut für Physik, Weimarer Str. 32, 98693 Ilmenau, Germany

[a] **Author to whom correspondence should be addressed:** kevin.lauer@tu-ilmenau.de

ABSTRACT

The piezo-resistive coefficient π_{44} is reported for the case of single crystalline *p*-type silicon. By comparing the measured sensitivity of pressure sensors with the simulated sensitivity of these pressure sensors, we are able to extract π_{44} since this is the only free parameter in the simulation. A value of $\pi_{44} = (108.3 \pm 2.1) \times 10^{-11}$ Pa^{-1} at a dopant concentration of $(5.0 \pm 4.5) \times 10^{17}$ cm^{-3} was found, which is in good agreement with experimental literature data.

I. INTRODUCTION

Pressure sensors based on silicon Micro-Electro-Mechanical Systems (MEMS) are widely used in industry for numerous applications.[1,2] A lot is known about MEMS pressure sensor design, manufacturing, and simulation.[3–6] The measured signal of such silicon based pressure sensors is often based on the piezo-resistive properties of silicon.[7] This means that an applied stress results in a change in the piezo-resistance of the silicon. Nevertheless, the underlying physical constants related to the piezo-resistivity in silicon, which have been obtained experimentally, have a rather large scatter.[8] However, to predict the output of a pressure sensor as exact as possible, the values of the physical constants must be known precisely. Therefore, we report the piezo-resistive coefficient π_{44}.

Mathematically, the piezo-resistivity can be described by a six-vector notation.[9] The stress vector σ_λ is connected via the piezo-resistivity tensor $\pi_{\kappa\lambda}$ to the change in resistivity vector $\Delta\rho_\kappa$,

$$\frac{\Delta\rho_\kappa}{\rho_0} = \pi_{\kappa\lambda}\sigma_\lambda, \tag{1}$$

with ρ_0 being the scalar resistivity without stress and $\kappa, \lambda = 1, \ldots, 6$. Due to the cubic crystal structure of silicon, the piezo-resistivity tensor has only three independent components π_{11}, π_{12}, and π_{44}, and the tensor is then

$$\pi_{\kappa\lambda} = \begin{pmatrix} \pi_{11} & \pi_{12} & \pi_{12} & 0 & 0 & 0 \\ \pi_{12} & \pi_{11} & \pi_{12} & 0 & 0 & 0 \\ \pi_{12} & \pi_{12} & \pi_{11} & 0 & 0 & 0 \\ 0 & 0 & 0 & \pi_{44} & 0 & 0 \\ 0 & 0 & 0 & 0 & \pi_{44} & 0 \\ 0 & 0 & 0 & 0 & 0 & \pi_{44} \end{pmatrix}. \tag{2}$$

In *p*-type silicon, the piezo-resistivity tensor component π_{44} is about two magnitudes larger than the other two components. Hence, the component π_{44} has the main impact on the resistivity change due to applied stress. Due to its importance, much effort[8] has been undertaken in the past to obtain the component π_{44} by experiment as well as by theory. Usually, test structures[8] or uniformly doped bars[10] are prepared, which are stressed, e.g., by a four point bending fixture.[8] The stress is calculated, and in consequence, π_{44} is calculated as well.

In this contribution, for the first time, the shear piezo-coefficient π_{44} is experimentally obtained by measuring the sensitivity of a pressure sensor. This sensitivity is simulated using the COMSOL Multiphysics® software package. The only free parameter

in this simulation is the shear piezo-coefficient π_{44}. This coefficient π_{44} is adapted in the simulation in a way that the measured sensitivity of the pressure sensor fits to the simulated sensitivity. In that way, the piezo-coefficient π_{44} is experimentally determined. The difference to previous studies is that a full featured pressure sensor is used with applied pressure to obtain the piezo-coefficient π_{44}.

II. EXPERIMENT

The schematic representation of the measured pressure sensor is shown in Fig. 1. Figure 1(a) shows a cross section of the pressure sensor, and Fig. 1(b) shows the top view of the pressure sensor. Black bars are the resistors. The pressure sensor consists of four resistors R_1 to R_4 placed on the edges of the membrane. The resistors themselves consist of boron doped bars with a size of $10 \times 100\ \mu m^2$ and a boron depth profile shown in Fig. 2. In Fig. 1(a), the cross section is shown for KOH etched membranes with tilted sidewalls.

The resistors are arranged in a Wheatstone bridge. The circuit diagram of this bridge is shown in Fig. 3. The output voltage U_O is calculated by knowing the resistors R_1 to R_4 and the supply voltage U_S in the following way:

$$U_O = U_S\left(\frac{R_1}{R_1 + R_2} - \frac{R_3}{R_3 + R_4}\right). \tag{3}$$

The pressure sensor is designed in a way that under pressure, $R_1 = R_4$ and $R_2 = R_3$ hold [see Fig. 1(b)]. It follows for the so-called

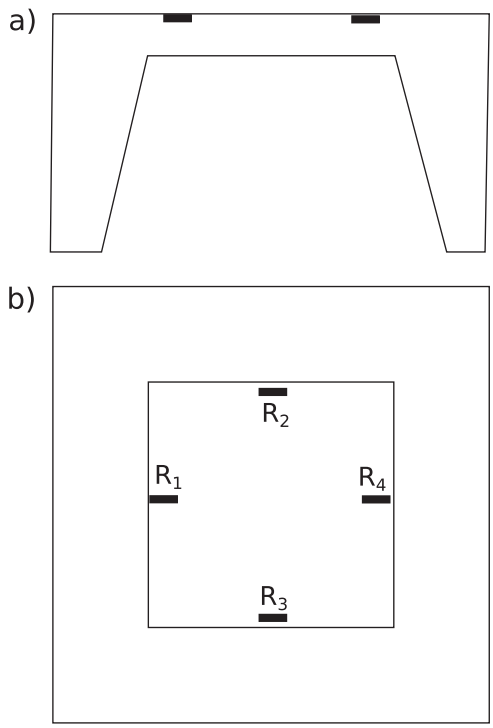

FIG. 1. Schematic representation of the measured pressure sensor. (a) Cross section and (b) top view.

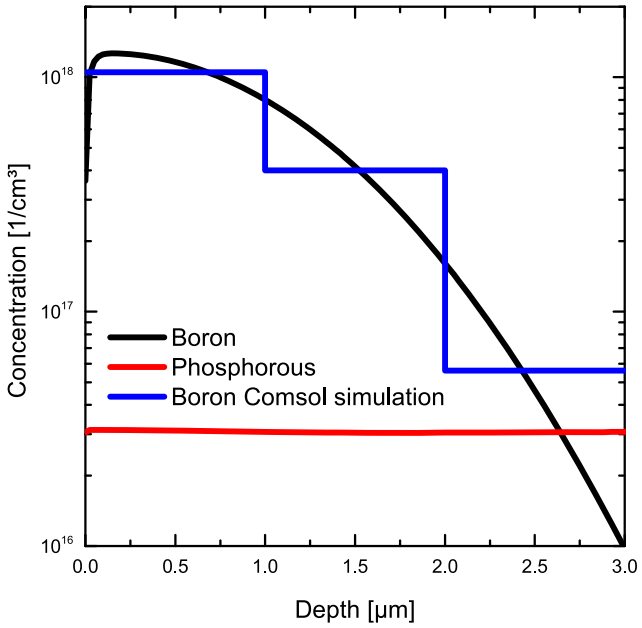

FIG. 2. Boron and phosphorous depth profiles (black and red lines) simulated by Atlas compared to the boron depth profile used for the COMSOL simulation of the resistors.

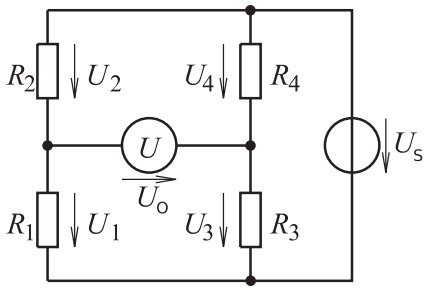

FIG. 3. Circuit diagram of a Wheatstone bridge.

sensitivity U_O/U_S given in (mV/V),

$$\frac{U_O}{U_S} = \left(\frac{R_1 - R_2}{R_1 + R_2}\right). \tag{4}$$

In the simulation, the resistance of the resistors R_1 and R_2 is obtained separately by applying Ohm's law $R_{1,2} = U_{1,2}/I_{1,2}$. This is done without using a Wheatstone bridge. A constant voltage $U_1 = U_2 = U$ is applied to R_1 and R_2, and the currents I_1 and I_2 are determined by COMSOL. Hence, we get

$$\frac{U_O}{U_S} = \left(\frac{I_2 - I_1}{I_1 + I_2}\right). \tag{5}$$

The sensitivity U_O/U_S is measured under applied pressure for the produced pressure sensors. Additionally, the currents I_1 and I_2 through the resistors are simulated by COMSOL under applied pressure.

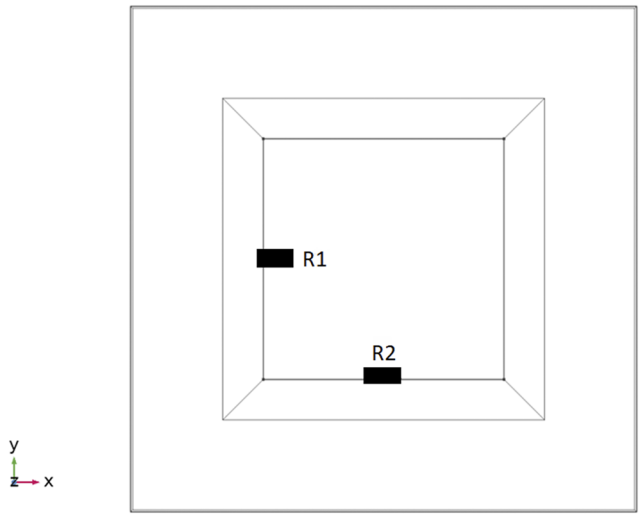

FIG. 4. Geometry of the simulated pressure sensor. Two simulated resistors R_1 and R_2 are clearly visible.

In the following, details about the simulation are given. Figure 4 shows the geometry of the simulated pressure sensor with its two resistors placed on the edge of the membrane. The membrane size is 2×2 mm^2. The geometry for the simulation follows the design of the produced pressure sensors. To save computation power, only the current through the resistors is simulated.

TABLE I. Standard parameters used for the simulation.[10–12]

Elastic constants (GPa)		Piezo-coefficients (10^{-11} Pa^{-1})	
C_{11}	166	π_{11}	6.6
C_{12}	64	π_{12}	−1.1
C_{44}	80		

The resistor itself consists of three bars, each $100 \times 10 \times 1$ μm^3 in size stacked one upon the other with different p-type doping. This is done to estimate the boron depth profile of the pressure sensor resistors. The depth profile of the simulated resistor is shown together with the boron depth profile in Fig. 2.

In Fig. 5, the mesh of the simulated pressure sensor is shown. The finer mesh in the region of the resistors is clearly visible.

A pressure of 50 kPa is applied to the membrane from the backside. The sensitivity is directly measured on the assembled pressure sensor. Several pressure sensors with different membrane thicknesses are used. The measurements are done at room temperature.

In the simulation, a pressure of 50 kPa is applied to the membrane as well. The mechanical behavior as well as the electric current is solved by the simulation simultaneously. The elastic constants[11,12] and the other piezo-coefficients[10] used for the simulation are the standard COMSOL parameters (see Table I). The simulation is straightforward. Anisotropic mode must be switched on, and a rotated coordinate system (+45°) must be defined for the elements (resistors, etc.).

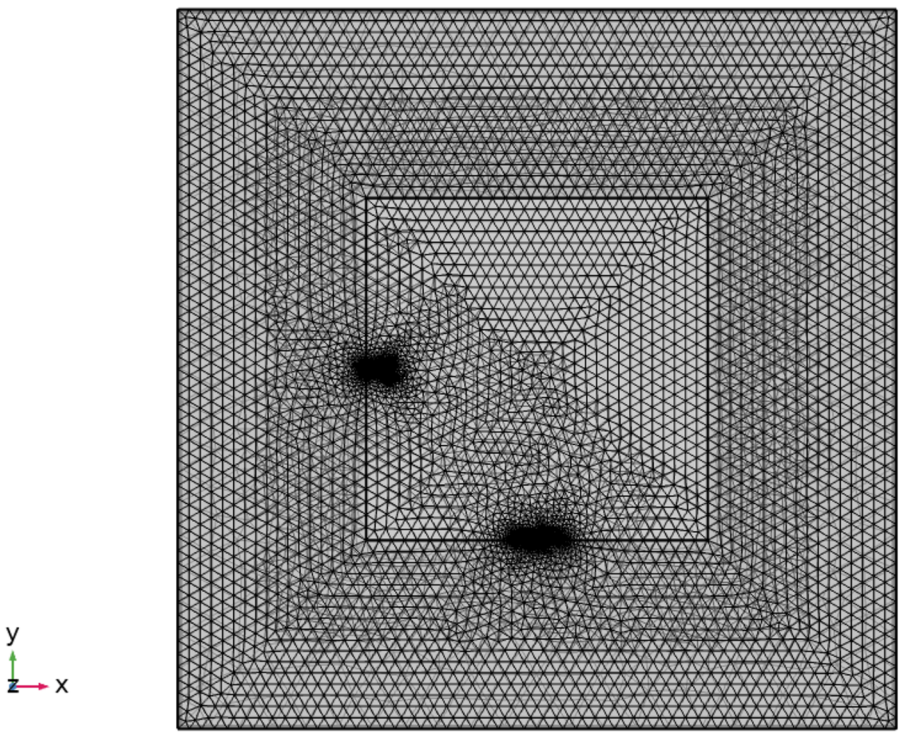

FIG. 5. Mesh of the simulated pressure sensor.

The currents I_1 and I_2 through the two resistors are obtained by applying a voltage. Using Eq. (5), the sensitivity is obtained from the simulated currents.

III. RESULTS

The results of the mechanical part of the simulation can be displayed spatially resolved as the stress components $\sigma_1 = \sigma_{xx}$ and $\sigma_2 = \sigma_{yy}$. In Fig. 6, the stress components σ_1 and σ_2 are depicted spatially resolved. The simulation is done for a 2 × 2 mm^2 membrane with a thickness of 30 μm under a pressure of 50 kPa. It is clearly visible that the maximum stress exists in the region where the resistors are placed.

The measured and simulated sensitivity is shown and compared in Fig. 7. The sensitivity is simulated for three different thicknesses of the membrane, 25, 30, and 35 μm. With decreasing membrane thickness, the sensitivity increases. The piezo-coefficient π_{44} is varied systematically from 104 × 10^{-11} to 114 × 10^{-11} Pa^{-1}. With the increasing piezo-coefficient, the sensitivity increases as well.

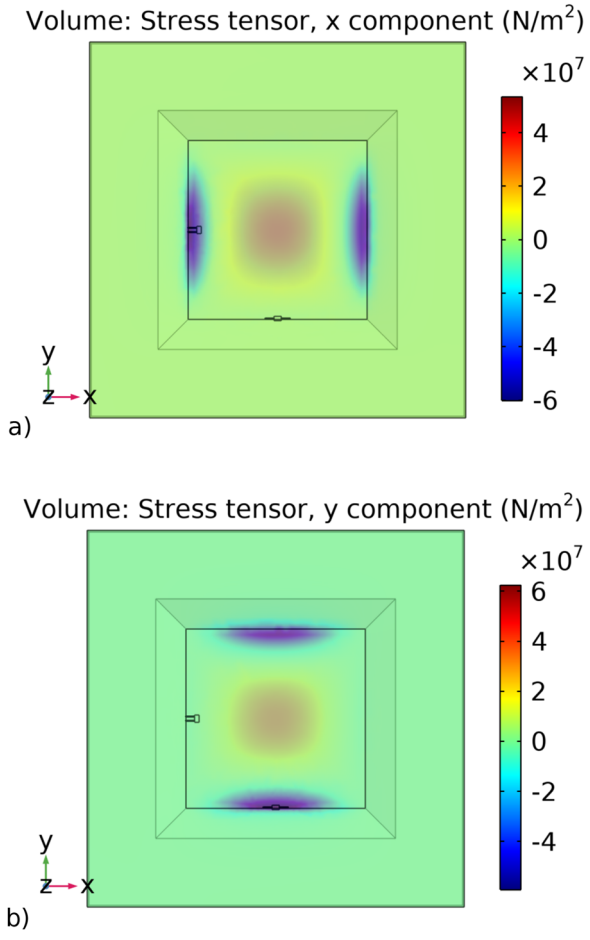

FIG. 6. Simulated stress components of a 2 × 2 × 0.03 mm^3 membrane under a pressure of 50 kPa. (a) $\sigma_1 = \sigma_{xx}$ and (b) $\sigma_2 = \sigma_{yy}$.

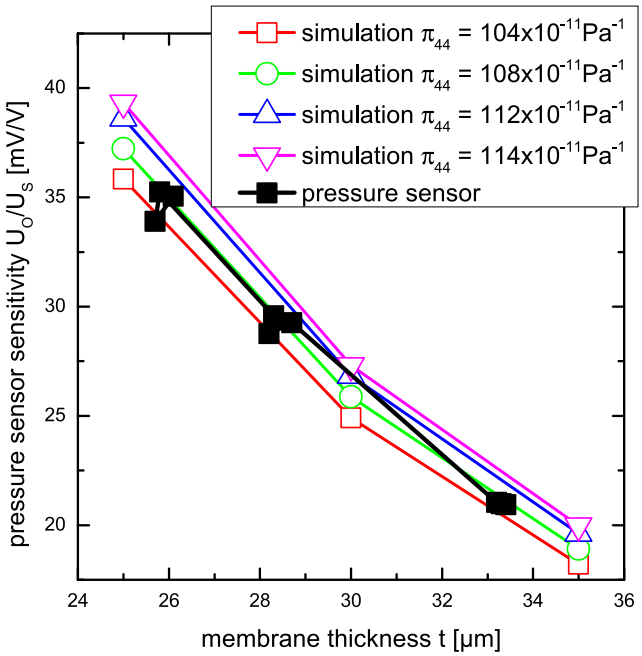

FIG. 7. Simulated and measured sensitivity of a pressure sensor for different thicknesses of the membrane. In the simulation, the piezo-resistive coefficient π_{44} is varied systematically.

For the determination of the sensitivity as a function of the membrane thickness, three different groups of pressure sensors are used. Each group has a different membrane thickness. A membrane thickness of ~26, ~28, and ~33 μm is used.

Obviously, the sensitivity is not a linear function of the membrane thickness t. The sensitivity is proportional to the inverse squared membrane thickness,[13,14]

$$U_O/U_S \sim 1/t^2. \quad (6)$$

Hence, the measured sensitivity as a function of the membrane thickness must be approximated by an inverse quadratic function. To estimate the measured sensitivity at a membrane thickness of 30 μm, an inverse quadratic function is fitted to the measured values. The result is depicted as the thick black line in Fig. 8. The thin black lines in Fig. 8 show the deviation of the measured sensitivity from the inverse quadratic fit function. In Fig. 8, the sensitivity for a membrane thickness of 30 μm is plotted as a function of the piezo-coefficient π_{44}. The simulation results are the red squares connected with a red line.

At the intersection of the measured and the simulated sensitivity, the piezo-coefficient π_{44} is determined. In this way, the piezo-coefficient $\pi_{44} = (108.3 \pm 2.1) \times 10^{-11}$ Pa^{-1} is obtained. The error of the piezo-coefficient π_{44} is determined from the intersection of the simulated sensitivity with the thin black lines, which represent the error of the measured sensitivity.

To compare the piezo-coefficient π_{44} obtained in this work to experimental literature data, we follow the collection of literature data of Richter *et al.*[8] These literature data from Refs. 10 and 15–19 are collected in Table II.

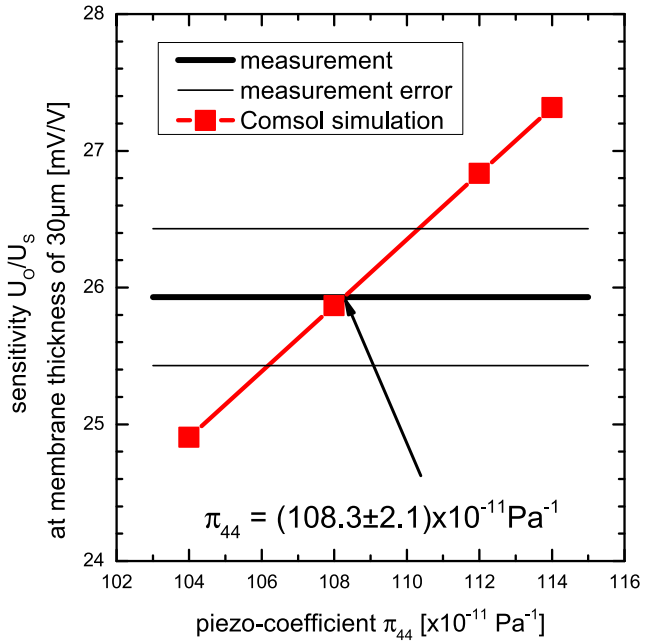

FIG. 8. The sensitivity at a membrane thickness of 30 μm is plotted as a function of the piezo-coefficient π_{44}. At the intersection of the measured value and the simulation, π_{44} is determined.

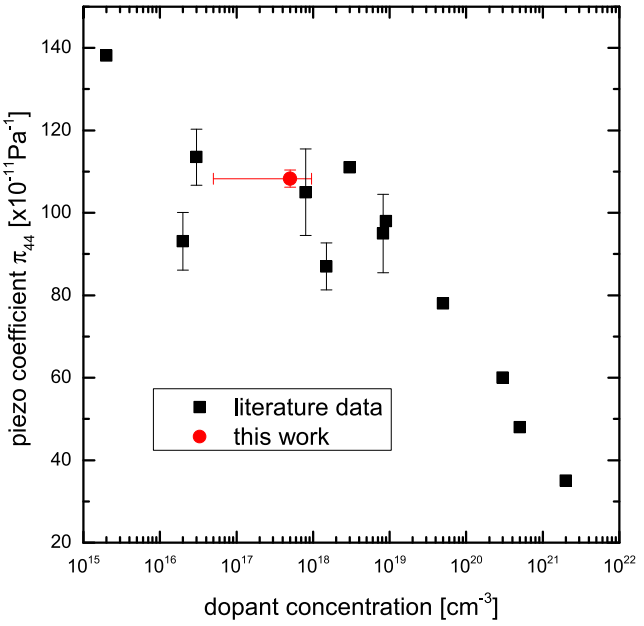

FIG. 9. Graphical comparison of the determined piezo-coefficient π_{44} with literature data.

TABLE II. Comparison of the determined piezo-coefficient π_{44} with literature data. Boldface denotes the piezo-coefficient obtained in this work.

References	Dopant density ($\times 10^{18}$ cm^{-3})	π_{44} ($\times 10^{-11}$ Pa^{-1})
10	0.002	138.1
15	0.02	93.1 ± 7.0
16	0.03	113.5 ± 6.8
This work	**0.50 ± 0.45**	**108.3 ± 2.1**
17	0.8	105 ± 10.5
18	1.5	87 ± 5.7
19	3	111
17	8.2	95 ± 9.5
19	9	98
19	50	78
19	300	60
19	500	48
19	2000	35

The literature data collected in Table II together with the piezo-coefficient obtained in this work are plotted in Fig. 9. The piezo-coefficient π_{44} is plotted as a function of the dopant concentration of the resistor. A decrease in the piezo-coefficient with the increasing dopant concentration is visible.

In our case, an average dopant concentration is used. We calculated the arithmetic average over the 3 μm thick resistor, which revealed an average boron concentration in the 3 μm of the resistor of (5.0 ± 4.5) × 10^{17} cm^{-3}. This is, in fact, a rough approximation of the real boron diffusion profile. However, since the current flows through all three resistor bars, it is a valid simplifying assumption. The current density differs by a factor of 9 between the bar with the highest doping level and the bar with the lowest doping level. The error is taken as the standard deviation of the three used dopant concentrations within the resistor. This is a very rough estimate too. However, the model applied here with a boron diffusion profile does not allow to state a more concrete average concentration value. To get a more concrete concentration value, a step like boron profile would be necessary for example.

In Fig. 9, it is clearly visible that there is a scatter in the literature data of π_{44} in the dopant concentration region where we obtained the piezo-coefficient π_{44}. Nevertheless, it can be stated that the piezo-coefficient π_{44} obtained in this work fits well to the reported values from the literature.

IV. CONCLUSIONS

In summary, we performed a study to estimate the piezo-coefficient π_{44} in silicon. Basically, π_{44} was obtained by comparing an experiment with simulation. Therefore, pressure sensors with different membrane thicknesses were built and the sensitivity in a Wheatstone bridge arrangement was measured. This sensitivity was simulated using the simulation software COMSOL Multiphysics. Therefore, the full pressure sensor with two resistors was simulated. The current through the resistors was extracted under an applied pressure, and the sensitivity was calculated. The simulations were done under systematic variation of the piezo-coefficient π_{44}. By comparing the sensitivity as a function of the piezo-coefficient π_{44} with the measured sensitivity, a value of π_{44} = (108.3 ± 2.1) × 10^{-11} Pa^{-1} at a dopant concentration of (5.0 ± 4.5) × 10^{17} cm^{-3} was found. This is in good agreement with the reported values from the literature.

Based on these results, it is now possible to predict the sensitivity of a pressure sensor more precisely.

ACKNOWLEDGMENTS

We acknowledge support for the publication costs from the Open Access Publication Fund of the Technische Universität Ilmenau.

DATA AVAILABILITY

The data that support the findings of this study are available from the corresponding author upon reasonable request.

REFERENCES

[1]V. Lindroos, *Handbook of Silicon Based MEMS Materials and Technologies* (William Andrew; Elsevier Science (distributor), Norwich, NY; Oxford, 2010), available at http://www.sciencedirect.com/science/book/9780815515944; accessed on March 18, 2014.

[2]S. Büttgenbach, I. Constantinou, A. Dietzel, and M. Leester-Schädel, "Piezoresistive pressure sensors," in *Case Studies in Micromechatronics: From Systems to Processes*, edited by S. Büttgenbach, I. Constantinou, A. Dietzel, and M. Leester-Schädel (Springer, Berlin, Heidelberg, 2020), pp. 21–85.

[3]S. S. Kumar and B. D. Pant, "Design principles and considerations for the 'ideal' silicon piezoresistive pressure sensor: A focused review," Microsyst. Technol. **20**(7), 1213–1247 (2014).

[4]A. V. Tran, X. Zhang, and B. Zhu, "The development of a new piezoresistive pressure sensor for low pressures," IEEE Trans. Ind. Electron. **65**(8), 6487–6496 (2018).

[5]H. Furlan, M. Fraga, L. Koberstein, and L. Rasia, "Modeling of MEMS piezoresistive sensors," in *Modelagem Matemática Aplicada à Resolução de Problemas nas Engenharias* (Unijui, 2012), pp. 215–240.

[6]X. Huang and D. Zhang, "A high sensitivity and high linearity pressure sensor based on a peninsula-structured diaphragm for low-pressure ranges," Sens. Actuators, A **216**, 176–189 (2014).

[7]A. A. Barlian, W.-T. Park, J. R. Mallon, A. J. Rastegar, and B. L. Pruitt, "Review: Semiconductor piezoresistance for microsystems," Proc. IEEE **97**(3), 513–552 (2009).

[8]J. Richter, J. Pedersen, M. Brandbyge, E. V. Thomsen, and O. Hansen, "Piezoresistance in *p*-type silicon revisited," J. Appl. Phys. **104**(2), 023715 (2008).

[9]J. Richter, Piezoresistivity in microsystems, available at https://orbit.dtu.dk/en/publications/piezoresistivity-in-microsystems, 2008.

[10]C. S. Smith, "Piezoresistance effect in germanium and silicon," Phys. Rev. **94**(1), 42–49 (1954).

[11]J. J. Hall, "Electronic effects in the elastic constants of *n*-type silicon," Phys. Rev. **161**(3), 756 (1967).

[12]C. S. G. Cousins, L. Gerward, J. Staun Olsen, B. Selsmark, and B. J. Sheldon, "Determination of internal strain tensors by energy-dispersive X-ray diffraction: Results for Si using the 006 forbidden reflection," J. Appl. Crystallogr. **15**(2), 154–159 (1982).

[13]C. Pramanik, H. Saha, and U. Gangopadhyay, "Design optimization of a high performance silicon MEMS piezoresistive pressure sensor for biomedical applications," J. Micromech. Microeng. **16**(10), 2060–2066 (2006).

[14]S. P. Timošenko and S. Woinowsky-Krieger, *Theory of Plates and Shells*, 2nd ed. (International edition) (McGraw-Hill, Auckland, 1976).

[15]R. E. Beaty, R. C. Jaeger, J. C. Suhling, R. W. Johnson, and R. D. Butler, "Evaluation of piezoresistive coefficient variation in silicon stress sensors using a four-point bending test fixture," IEEE Trans. Compon., Hybrids, Manuf. Technol. **15**(5), 904–914 (1992).

[16]R. C. Jaeger, J. C. Suhling, and A. A. Anderson, "A [100] silicon stress test chip with optimized piezoresistive sensor rosettes," in *Proceedings of the 44th Electronic Components and Technology Conference, May 1994* (IEEE, 1994), pp. 741–749.

[17]E. Lund and T. Finstad, "Measurement of the temperature dependency of the piezoresistance coefficients in p-type silicon," in *InterPACK '99: Pacific RIM/ASME International Intersociety Electronics Photonic Packaging Conference* (ASME, 1999), pp. 215–218.

[18]R. C. Jaeger, J. C. Suhling, M. T. Carey, and R. W. Johnson, "Off-axis sensor rosettes for measurement of the piezoresistive coefficients of silicon," IEEE Trans. Compon., Hybrids, Manuf. Technol. **16**(8), 925–931 (1993).

[19]O. N. Tufte and E. L. Stelzer, "Piezoresistive properties of silicon diffused layers," J. Appl. Phys. **34**(2), 313–318 (1963).